Volume 9, Issue 2, 2020, 995 - 999 **ISSN 2284-6808**

Letters in Applied NanoBioScience

https://nanobioletters.com/

https://doi.org/10.33263/LIANBS92.995999

Original Research Article **Open Access Journal**

Received: 10.04.2020 / Revised: 03.05.2020 / Accepted: 06.05.2020 / Published on-line: 10.05.2020

Nanocomposite hydrogel of chitosan-g-poly acrylamide/ nanoclay: effect of degree of cross-linking on their swelling

Kazem Tajdini [1], Alireza Shakeri [2,*], Fatemeh Naijian [3]

[1] Department of Chemistry, Faculty of Sciences, Golestan University, P.O. Box: 49138-15759, Gorgan,Iran
[2] School of chemistry, University College of Science, University of Tehran, P.O. Box 13145-1357, Tehran, Iran
[3] Department of Biorefinery Engineering, Faculty of New Technologies and Energy Engineering, Shahid Beheshti University, Zirab, Mazandaran, Iran
*corresponding author e-mail address: ***alireza.shakeri@ut.ac.ir,*** Scopus ID 57197226439

ABSTRACT

In this study a chitosan-g-Polyacrylamide hydrogel was prepared through graft copolymerization in the presence of an appropriate amount of potassium persulfate as the initiator and different ratio of methylene bis acrylamide as the crosslinker agent. After dewatering the gels in acetone and being dried in oven, the swelling behaviors of hydrogels in different media such as distilled water, NaCl 0.15M, basic buffer with pH=10 and acidic buffer with pH=3 were evaluated. The gel with the highest swelling degree (i.e. 1/60 crosslinker) was selected to be used in the synthesis of nanocomposite hydrogel. Nanocomposite hydrogels with 1, 3, 5 percent of nanoclay were synthesized respectively. Swelling behaviors of nanocomposite hydrogels were examined. The results of swelling test showed a decrease in the swelling extent as the crosslinker ratio is increased. The result showed that different swelling behaviors as the media of experiment is changed. They showed a lower swelling extent in saline media than in distilled water. The results of swelling test in buffer media show lower swelling extent than in distilled water and swelling extent in acidic buffer with pH=3 is greater than swelling extent in basic buffer with pH=10. The swelling extent of nanocomposite increases slightly with the increase of nanoclay content up to 1%. More increase in the nanoclay content caused a drastic decrease in the swelling extent as well.

Keywords: *hydrogel; nanocomposite; nanoclay; chitosan; acrylamide; swelling.*

1. INTRODUCTION

Today polymer hydrogel have many applications in various processes such as pharmacy, medicine and agriculture applications [1]. Hydrogel is defined as a crosslinked three-dimensional polymeric network structure, which can absorb and retain considerable amount of water,in other words, hydrogels are water-swollen polymer network [2, 3]. Hoffman presented another definition of hydrogel, which according to this definition hydrogels are considered as a permanent or chemical gel crosslinked by covalent bonds [4]. These chemically made hydrogels could be fabricated either by cross-linked polymer chains that are composed of three-dimensional network s. The ability of large amounts of water absorptions and the swelling properties and as a consequence behaving similarly to soft tissues are result of many polar and hydrophilic functional groups (i.e. hydroxyl, ammonium, carboxyl, and sulphonic acid) in the structure of polymer hydrogels, is the reason why polymer hydrogels absorb a large amount of water.The water content in hydrogels encompasses a wide range of amounts starting from detailed values to high percentages- up to 99%- retaining the properties of solids [5,6]. The restriction of these super absorbents' wide application is because of their high production expenses and on the other hand, their low gel strength. By using inorganic compounds which cost lower, we can improved such restriction [7]. Hybrid hydrogels which are clay-based because thenatural clays are abundantly available low-cost natural resource which is nontoxic and cheap material [8]. Medical toughness, large deformability, high rates of swelling/ deswelling, and high transparency is of nanocomposite hydrogel's properties, which are due to their characteristic network structure [9-11]. The crosslink density of hydrogel is closely related to physical and mechanical properties such as mechanical strength and permeability. The mechanical properties of hydrogels depend on their composition and structures. The fully swollen hydrogel are low mechanical strength, this properties can be improved by increasing cross-linking density, nanoparticles, making an interpenetrating network (IPN) structure or copolymerization with other monomers [12]. Along the polymer back bone there are some special functional groups which cause them sensitivity to the environment conditions such as temperature, pH, ionic strength of the swelling solutions or the presence of a magnetic field or ultraviolet light. Attention has been directed toward hydrogel polymers being prepared through graft copolymerization of vinyl monomers onto natural polymer chains such as starch, cellulose, and chitosan(CS) [13-16]. Hydrogels based on chitosan-g-poly acrylamide and reinforced with nanoclay or montorillonite have been developed previously [16, 17]. The aim of present work is to synthesize chitosan-g-Polyacrylamide hydrogel in the presence of an appropriate amount of potassium persulfate as the initiator and different ratio of methylene bis acrylamide as the crosslinker agent. Swelling behavior of these hydrogel systems in distilled water, buffer and NaCl solutions has been studied. In addition, the swelling response of hydrogel against the different amount of nanoclay has also been studied in detail.

2. MATERIALS AND METHODS

2.1. Materials.

Modified clay (Cloisite®15A) nano particles were purchased from Southern Clay Company. Chitosan(CS) (medium molecular weight, 75–85% deacetylated, Sigma-Aldrich), acetic acid (HPLC, TEDIA), Acryleamide (AAm Merck), potassium persulfate (PS, Merck) Methylene bis acrylamide (MBA, Merck) dissolved in DI water and were used to prepare polymer hydrogel. Sodium hydroxide, sodium chloride, sodium hydrogen carbonate, hydrochloric acid were purchased from Merck. Ethanol (90%) was bought from Dr.Mojallali Company and Potassium hydrogen phthalate was provided by Panreac Appli Chem Company.

2.2. Hydrogels preparation.

CS solution was prepared in a 100ml beaker equipped with a mechanical stirrer and an inert gas inlet (nitrogen). CS was dissolved in degassed, distilled water containing 1 wt% of acetic acid. In general, 0.50 g of CS was dissolved in 50.0 mL of the acetic acid solution. The reactor was placed in a water bath preset at 60°C. Then 0.10 g of PS was added to the CS solution and the resulting mixture was stirred for 10 min at 60°C. Following this procedure, 2.0g AAm was added to the CS solution. MBA (1/60,1/30,1/20,1/10,1/5 to AAm weight) as a cross linker was added to the reaction mixture. After the addition of monomer, the mixture was continuously stirred at a temperature of 60 °C for 1 h under nitrogen atmosphere. Subsequently, the resulting hydrogels were immersed in ethanol and the ethanol was repeatedly changed every 8 h to 24 h in order to remove the soluble impurities in the hydrogel. As-resulted nanocomposite hydrogel was filtered and dried at 60 °C for 12 h.

2.3. Preparation of nanocomposite hydrogels.

Nanocomposite hydrogels were prepared by free-radical polymerization of solutions composed of AAm, as monomers, nanoclay as modifiers, MBA as a cross linker, and PS as a redox initiator. Various amounts of dried nanoclay (1,3,5 wt% to acrylamide weight) was suspended in 50 mL 1 wt% acetic acid solution in a 100 ml three-neck flask equipped with ultrasound waves and the mixture was strried for 24 h and sonicated for 15 min in order to make a homogeneous suspantion of nanoclay. Then 0.5 g of CS was dissolved in solution. Nanocomposite hydrogel were synthesized similar to the described method, without nanoclay incorporation.

2.4. Instrumental analysis

The FTIR spectrum of polymer hydrogel was achieved on a Bruker, Tensor 27 (Bruker, Germany). The surface morphology of the polymer hydrogel was investigated by using scanning electron microscopy (FE-SEM). Dried polymer hydrogel powder was coated with a thin layer of gold and image was achieved by FE-SEM technique (FE-SEM, HITACHI S4160, Japan). X-ray diffraction (XRD) patterns were achieved using (Philips, PW1730, Netherland) X-ray diffractometer at a tube voltage of 40 kV, and a tube current of 30 mA. The XRD patterns were recorded with a step size of 0.04 from 2Θ = 5 to 10.

2.4.4. Swelling measurements.

The conventional tea-bag technique was employed to explore the swelling performances of nanocomposite hydrogels. 0.05 g of polymer hydrogel was put into a dialysis bag and immersed in 100 mL of deionized water and allowed to immerse for 72 h at room temperature to reach equilibrium. The swelling ratio (S) of polymer hydrogels was calculated as follows:

$$S(\%) = \frac{W_s - W_d}{W_d} \times 100$$

where W_s and W_d are the weight of the hydrogel after swelling (g) and the weight of the dried hydrogel (g). Pure polymer hydrogels were evaluated in two buffer solutions (pH=3 ($KC_8H_5O_4$ / HCl) and pH=10 ($NaHCO_3$/ NaOH) solution) and 0.15 M aqueous solutions of NaCl similar to the described method.

3. RESULTS

The intense absorption band at 3430 cm^{-1} is attributed to NH stretching band of acrylamide, which is shown in the FT-IR spectra of CS graft polyacrylamide hydrogel (Fig. 1). The NH and OH absorption bands of CS form a shoulder on the peak at about 3200 cm^{-1} that confirms graft reaction of polyacrylamide on the CS. The second intense absorption band at 1662 cm^{-1} is attributed to overlapped bands of amine bending vibration and carbonyl stretching vibrations in polyacrylamide chains. The amide type (I) bonding of CS is seen as a shoulder on the peak at about 1590 cm^{-1}, which further supports the grafting reaction [14].

3.1. FT-IR spectra of nanocomposite hydrogel.

FT-IR spectra of nanocomposite hydrogels (Figure 2), represents the chemical interaction between the hydrogel molecules and nanoclay particles. From the FT-IR spectra of pure components and nanocomposite hydrogels it can be observed that the intensity of –OH absorption band is lower in the hydrogels as compared to –OH stretching vibration band CS graft polyacrylamide hydrogel and nanoclay. Shifting some peaks to another bands, for instance shifting the –OH band stretch for Si–OH from 3698cm^{-1} to 3749cm^{-1}, –OH bending mode in water (adsorbed water) from 1640cm^{-1} to 1610cm^{-1}, Si–O stretching (out-of-plane) from 1115cm^{-1} to 1065cm^{-1}, quartz from 692cm^{-1} to 694cm^{-1} and reduction the intensities of peaks in the range of 725cm^{-1} to 429cm^{-1} witch attributed to metal oxides M-O.

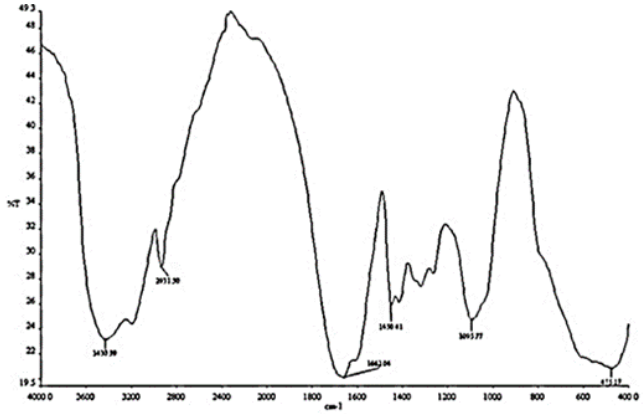

Figure 1. FT-IR spectra of CS graft polyacrylamide hydrogel.

3.2. X-ray diffraction.

For the dispersion determination of nano silicates as well as determining the structure, X-Ray diffraction was used. According to the Bragg's equation (λ=2dsinθ) every basal spacing of nano platelets shows a diffraction angle that can be related to the

appeared peaks. As figure 3 illustrates, pristine Na+-MMT shows diffraction peak at about 7.4° corresponds to the basal spacing of 1.17nm. The increase of pure clay's interlayer space is a result of polymer chain incorporation [18].

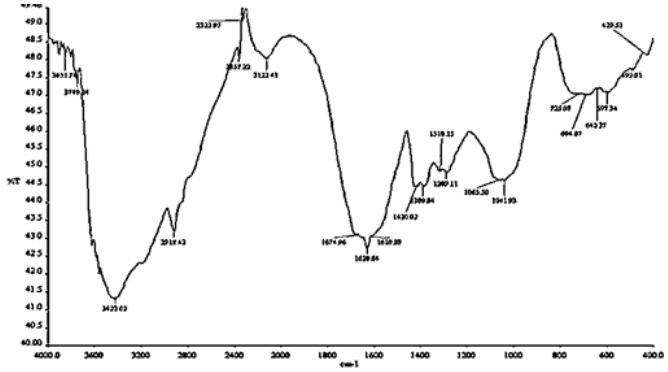

Figure 2. FT-IR spectra of nanocomposite hydrogel.

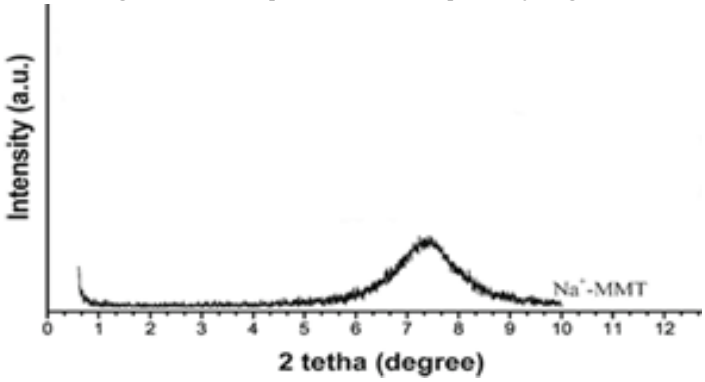

Figure 3. X-ray diffraction of pristine montmorilonite hydrogel.

In Figure 4, the X-ray diffraction pattern of nanocomposite hydrogel with 1 wt% of nanoclay is presented. To prove that polymer chains are located between clay's layers and the fact that particle's layers are separated and dispersed in the gel matrix, we can cite the lack of any distinguishable peak in the XRD patterns of nanocomposite hydrogel, so that the exfoliated structure is justifiable.

3.3. FE-SEM.

Figure 5 (A) illustrates the FE-SEM image of cross-section morphology of CS-polyacrylamide hydrogel without nanoclay. The image shows a smooth surface because of the homogeneity of their structure and so there are as such no barriers to stop this smooth propagation.

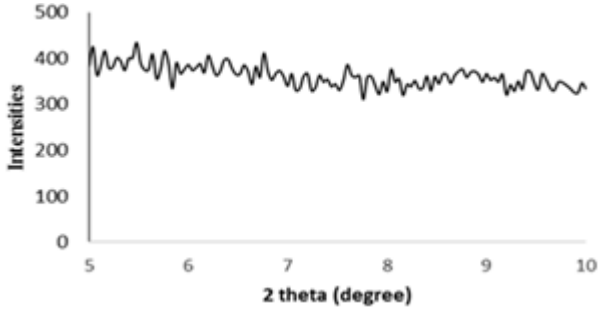

Figure 4. X-ray diffraction of nanocomposite.

Figure 5 (B) illustrates the FE.SEM image of cross-section morphology of a nanocomposite hydrogel with 1 wt% nanoclay. The complete attachment of particles to the gel matrix and the absence of non-occupied micro-voids and agglomerates of the polymer chain as well, are results of nanoclay particles' good dispersion which is shown in the image. Furthermore, the significant increase of surface's roughness and destruction of the smooth surface is observed. This observation shows the exfoliated structure of hydrogel nanocomposite and confirms with XRD results.

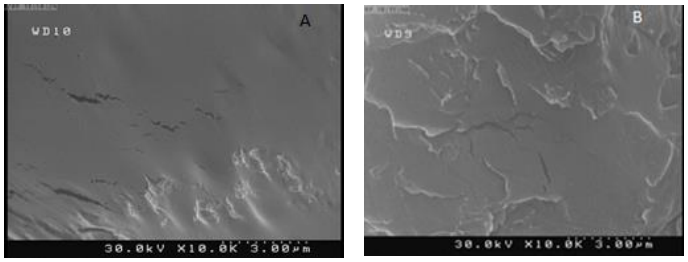

Figure 5. FESEM image of cross-section of hydrogel without clay (A) and with 1wt% nanoclay (B).

3.4. Swelling results.

The results of hydrogels swelling are presented in table 1. As the concentration of MBA was increased, the water absorbency of hydrogels decreased, so that the hydrogel with 1/60 MBA (to acryleamide monomer weight ratio) has the maximum swelling content and the hydrogel with 1/5 MBA (to acryleamide monomer weight ratio) has the minimum swelling content.

Table 1. Results of hydrogels swelling in distilled water.

MBA to AAM ratio	1/5	1/10	1/20	1/30	1/60
swelling (g/g)	8.67	13.05	15.16	17.95	23.40

A decrease in the swelling rate especially when it is in contact with the solvents is a result of the higher extent of crosslinking of the polymer network, which is because of the use of larger amounts of crosslinker's concentration [19-20]. The related chart is shown in figure 6. The curve shows the power law behavior. The power law coefficient is 4.95 and its power is 0.38. The swelling extents in 0.15M NaCl solution are appreciably decreased compared to the values measured in distilled water (table 2).

Table 2. Swelling in 0.15 M NaCl solution.

MBA to AAM ratio	1/5	1/10	1/20	1/30	1/60
swelling (g/g)	8.05	10.60	12.80	16.45	22.10

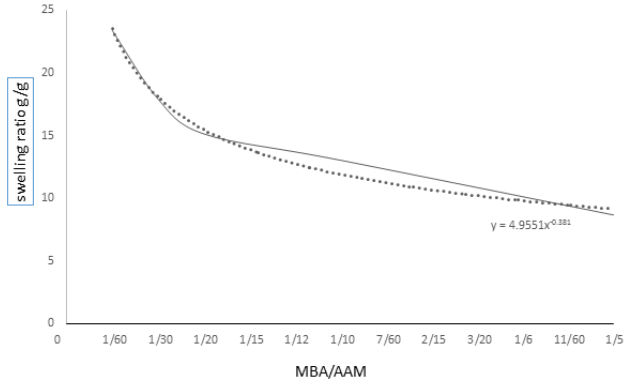

Figure 6. Effect of crosslinker concentration on swelling behaviour of hydrogel.

The anion-anion electrostatic repulsion which is resulted by the screening effect of additional cations, causes this phenomenon, which most of the time is observed when ionic hydrogels swell. As a consequence the osmotic pressure (ionic pressure) between the hydrogel network and the external solution is decreased [21]. The

related chart shows power law behavior (figure 7). The power law coefficient is 4.13 and its power is -0.40.

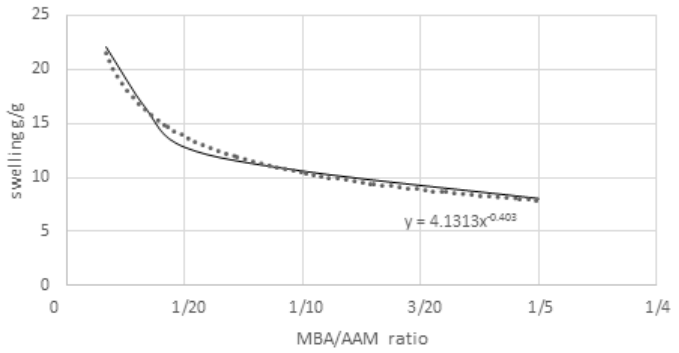

Figure 7. Swelling in 0.15M NaCl solution.

The swelling extends for the samples to have the maximum value in distilled water (table 3). This is due to the higher ionic strength of the buffer solutions. The swelling values in acidic buffer (pH=3) are more than those in basic buffer (pH=10) (table 3). The NH4+ – NH4+ electrostatic repulsion causes an enhancement of the osmotic pressure inside the gel particles which is a result of the increase of polymer charge density because of the presence of NH4+.

Table 3. Swelling extents in buffer solutions.

MBA to AAM ratio	1/5	1/10	1/20	1/30	1/60
swelling (g/g) pH=3	8.36	10.56	13.10	18.20	22.80
Swelling (g/g) pH=10	7.34	9.10	11.60	15.40	21.20

There is an osmotic difference between the internal and external solutions which makes the water absorption of gel to be a little bit larger. The swelling behavior is limited at pH 10 because of the screening effect of the counter ions (Na+) [22]. The charts of swelling in two buffer solution are shown in figure 8. The curve shows power law behavior. The acidic buffer power law coefficient is 4.14 and its power is-0.41. The basic buffer, power law coefficient is 3.47 and its power is -0.43.

Hydrogel with 1/60 ratio MBA to acrylamide was selected. Nanocomposite hydrogels with 1, 3, 5 wt% nanoclay were synthesized. Swelling behavior of Nanocomposite hydrogels were examined in distilled water and the results are shown in Table 4. The results reveal that the swelling capacity is enhanced by increasing the nanoclay content up to 1wt % of nanoclay content. The increase in the osmotic pressure of nanocomposites causes an increase in the swelling rate. This osmotic pressure is due to the mobility of ions on the nanoclay particles [23].

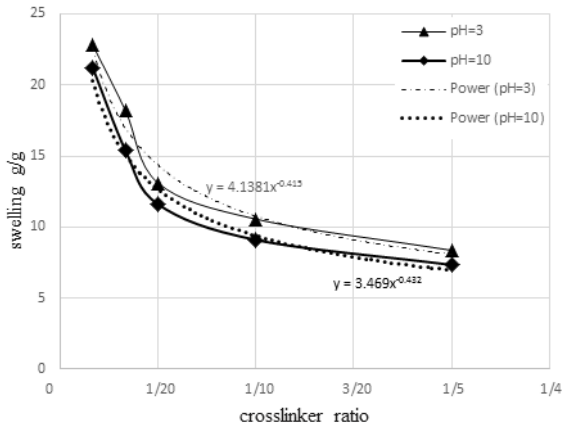

Figure 8. Effect of pH on swelling in buffer media.

Table 4. Effect of nanoclay content on swelling behavior in distilled water.

Nanoclay (%)	0	1	3	5
swelling (g/g)	16.85	17.06	13.88	10.60

Further increase in nanoclay content leads to a decrease in the swelling capacity. This phenomenon may be attributed to the fact that the MMT can act as an additional cross-linking point in the polymeric network to decrease the elasticity of polymers. Additionally, the excess of MMT would also decrease the hydrophilicity as well as the osmotic pressure difference, resulting in shrinkage of the composite [24]. The swelling behavior chart is shown in Figure 9.

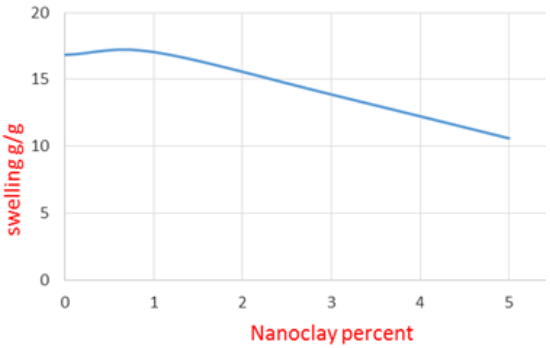

Figure 9. Effect of nanoclay content on swelling behavior in distilled water.

4. CONCLUSIONS

The chitosan-g-acrylamide hydrogel was synthesized by free radical co-polymerization. The swelling behavior was determined in distilled water and salt solutions and basic and acidic buffers. The gel had a pH dependent swelling behavior which showed higher swelling rate in acidic buffer pH=3 than pH=10. The swelling behavior also depends on crosslinker ratio and in reverse order by swelling content. The swelling value in NaCl 0.15M was lower than in distilled water. The effect of nanoclay content (in 1, 3, 5 wt %) on swelling of nanocomposite hydrogels were also examined. Increasing nanoclay content up to 1 wt% caused an increase in the swelling content. Further increase in nanoclay content decreases the swelling capacity

5. REFERENCES

1. Ullah, F.; Othman, M.B.H.; Javed, F.; Ahmad, Z.; Akil, H.M. Classification, processing and application of hydrogels: A review. *Materials Science and Engineering: C* **2015**, *57*, 414-433, https://doi.org/10.1016/j.msec.2015.07.053.
2. Pellá, M.C.; Lima-Tenório, M.K., Tenório-Neto, E.T., Guilherme, M.R.; Muniz, E.C.; Rubira, A.F. Chitosan-based hydrogels: From preparation to biomedical applications. *Carbohydrate Polymers* **2018**, *196*, 233-245, https://doi.org/10.1016/j.carbpol.2018.05.033.
3. Wang, W.; Wang, J.; Zhao, Y.; Bai, H.; Huang, M.; Zhang, T.; Song, S. High-performance two-dimensional montmorillonite supported-poly (acrylamide-co-acrylic acid) hydrogel for dye

removal. *Environmental Pollution* **2020**, *257*, https://doi.org/10.1016/j.envpol.2019.113574.
4. Hoffman, A.S. Hydrogel biomedical articles. *Adv. Drug Deliv. Rev* **2002**, *54*, 3-12, https://doi.org/10.1016/j.addr.2012.09.010.
5. Appel, E.A.; Loh, X.J.; Jones, S.T.; Biedermann, F.; Dreiss, C.A.; Scherman, O.A. Ultrahigh-water-content supramolecular hydrogels exhibiting multistimuli responsiveness. *Journal of the American Chemical Society* **2012**, *134*, 11767-11773, https://doi.org/10.1021/ja3044568.
6. Wang, Q.; Mynar, J.L; Yoshida, M.; Lee, E.; Lee, M.; Okuro, K.; Aida, T. High-water-content mouldable hydrogels by mixing clay and a dendritic molecular binder. *Nature* **2010**, *463*, 339-343, https://doi.org/10.1038/nature08693.
7. Gu, H.; Zhang, H.; Ma, C.; Sun, H.; Liu, C.; Dai, K.; ... Guo, Z. Smart strain sensing organic–inorganic hybrid hydrogels with nano barium ferrite as the cross-linker. *Journal of Materials Chemistry C* **2019**, *7*, 2353-2360, https://doi.org/10.1039/c8tc05448g.
8. Bagheri Marandi, G.; Mahdavinia, G.R.; Ghafary, S. Swelling behavior of novel protein-based superabsorbent nanocomposite. *Journal of Applied Polymer Science* **2011**, *120*, 1170-1179, https://doi.org/10.1002/app.33016.
9. Huang, S.; Yang, L.; Liu, M.; Phua, S. L.; Yee, W. A.; Liu, W.; Lu, X. Complexes of polydopamine-modified clay and ferric ions as the framework for pollutant-absorbing supramolecular hydrogels. *Langmuir* **2013**, *29*, 1238-1244.
10. Rafieian, S.; Mirzadeh, H.; Mahdavi, H.; Masoumi, M. A review on nanocomposite hydrogels and their biomedical applications. *Science and Engineering of Composite Materials* **2019**, *26*, 154-174, https://doi.org/10.1515/secm-2017-0161.
11. Shah, L.A.; Khan, M.; Javed, R.; Sayed, M.; Khan, M.S.; Khan, A.; Ullah, M. Superabsorbent polymer hydrogels with good thermal and mechanical properties for removal of selected heavy metal ions. *Journal of cleaner production* **2018**, *201*, 78-87, https://doi.org/10.1016/j.jclepro.2018.08.035.
12. Perera, D.I.; Shanks, R.A. Swelling and mechanical properties of crosslinked hydrogels containing N-vinylpyrrolidone. *Polymer international* **1996**, *39*(2), 121-127, https://doi.org/10.1002/(SICI)1097-0126(199602)39:2%3C121::AID-PI477%3E3.0.CO;2-8.
13. Shakeri, A.; Salehi, H.; Nakhjiri, M.T.; Shakeri, E.; Khankeshipour, N.; Ghorbani, F. Carboxymethylcellulose-quaternary graphene oxide nanocomposite polymer hydrogel as a biodegradable draw agent for osmotic water treatment process. *Cellulose* **2019**, *26*(3), 1841-1853, https://doi.org/10.1007/s10570-018-2153-0, .
14. Hamedi, H.; Moradi, S.; Hudson, S.M.; Tonelli, A.E. Chitosan based hydrogels and their applications for drug delivery in wound dressings: A review. *Carbohydrate polymers* **2018**, *199*, 445-460, https://doi.org/10.1016/j.carbpol.2018.06.114.
15. Lu, J.; Zhu, W.; Dai, L.; Si, C.; Ni, Y. Fabrication of thermo- and pH-sensitive cellulose nanofibrils-reinforced hydrogel with biomass nanoparticles. *Carbohydrate polymers* **2019**, *215*, 289-295, https://doi.org/10.1016/j.carbpol.2019.03.100.
16. El-Hoshoudy, A.N. Synthesis of acryloylated starch-g-poly acrylates crosslinked polymer functionalized by emulsified vinyltrimethylsilane derivative as a novel EOR agent for severe polymer flooding strategy. *International journal of biological macromolecules* **2019**, *123*, 124-132, https://doi.org/10.1016/j.ijbiomac.2018.11.056.
17. Olad, A.; Zebhi, H.; Salari, D.; Mirmohseni, A.; Reyhanitabar, A. A promising porous polymer-nanoclay hydrogel nanocomposite as water reservoir material: synthesis and kinetic study. *Journal of Porous Materials* **2018**, *25*, 665-675, https://doi.org/10.1007/s10934-017-0479-x.
18. Ghelichi, M.; Qazvini, N.T.; Jafari, S.H.; Khonakdar, H.A.; Reuter, U. Nanoclay dispersion in a miscible blend: an assessment through rheological analysis. *Journal of Polymer Research* **2012**, *19*, 9830-9838, https://doi.org/10.1007/s10965-012-9830-8.
19. Wu, J.; Lin, J.; Li, G.; Wei, C. Influence of the COOH and COONa groups and crosslink density of poly (acrylic acid)/montmorillonite superabsorbent composite on water absorbency. *Polymer International* **2001**, 50, 1050-1053, https://doi.org/10.1002/pi.728.
20. Wong, R.S.H.; Ashton, M.; Dodou, K. Effect of crosslinking agent concentration on the properties of unmedicated hydrogels. *Pharmaceutics* **2015**, *7*, 305-319, https://doi.org/10.3390/pharmaceutics7030305.
21. Wang, H.; Wei, J.; Simon, G.P. Response to osmotic pressure versus swelling pressure: comment on bifunctional polymer hydrogel layers as forward osmosis draw agents for continuous production of fresh water using solar energy. *Environmental science & technology* **2014**, *48*, 4214-4215.
22. Mahdavinia, G.R.; Pourjavadi, A.; Hosseinzadeh, H.; Zohuriaan, M.J. Modified chitosan 4. Superabsorbent hydrogels from poly (acrylic acid-co-acrylamide) grafted chitosan with salt-and pH-responsiveness properties. *European Polymer Journal* **2004**, *40*, 1399-1407, https://doi.org/10.1016/j.eurpolymj.2004.01.039.
23. Li, A.; Zhang, J.; Wang, A. Preparation and slow-release property of a poly (acrylic acid)/attapulgite/sodium humate superabsorbent composite. *Journal of applied polymer science* **2007**, 103, 37-45, https://doi.org/10.1002/app.23901.
24. Wu, L.; Liu, M. Slow-release potassium silicate fertilizer with the function of superabsorbent and water retention. *Industrial & engineering chemistry research* **2007**, *46*, 6494-6500.